

## Studies on triple junction electric field in ferroelectric cathodes

Meduri Ravi\* & K S Bhat

Microwave Tube Research & Development Centre,  
Defence Research & Development Organization, Bangalore 560 093, India

Received 4 September 2016; accepted 31 October 2017

To investigate the effect of grid thickness and dielectric constant on the ferroelectric cathode triple junction electric field distribution in a two-dimensional structure, simulation has been carried out using finite element method (FEM) code ANSYS. Triple junction electric field plays a major role in the emission of electrons from a ferroelectric cathode and it approaches towards its limiting value even if the dielectric constant of the ferroelectric material is increased considerably. It is important to increase the triple junction electric field without increasing the applied field to reduce the mechanical stresses in the ferroelectric material. A dielectric layer ( $\epsilon_r < 100$ ) has been introduced between the ferroelectric material and the grid to increase the triple junction electric field. FEM simulation results showed that the triple junction electric field is more than 48 times the applied field in this case. This structure not only enhances the triple junction electric field but it also changes the  $E_{\parallel}$  and  $E_{\perp}$  ratio ( $\beta$ ) favorably. Effects of dielectric constant and the thickness of the dielectric layer on triple junction electric field have been studied.

**Keywords:** Electron emission, Ferroelectric cathodes, Field enhancement, Triple point junction

### 1 Introduction

Ferroelectric cathodes became attractive for use in vacuum electron devices. It is reported by various groups that more than  $100 \text{ A/cm}^2$  current density can be achieved from ferroelectric cathodes and a feature common to all these cathodes is the patterned front electrode<sup>1-3</sup>. Rosenman *et al.*<sup>1</sup> observed that weak electron emission has been studied in “plane to plane” geometry without strip-patterned electrode. It can be assumed that the specific geometry of the front electrode is a key factor leading to the strong electron emission from ferroelectric cathodes. This motivates the modeling of electric field distribution in a typical ferroelectric cathode experimental set up with a grid patterned front electrode. Typical configuration of ferroelectric cathode for strong electron emission is with a grid of strip width and the distance between the strips of  $200 \mu\text{m}$ . The thickness of the ferroelectric sample is 1 mm.

To understand the effect of grid on the emitting surface of the grid several studies have been carried out by various researchers. Schachter<sup>4</sup> studied the triple point electron emission from an ideal edge analytically. Heydari and Tille<sup>5</sup> also studied electric field enhancement in ferroelectric cathodes using

theoretical model. Chung *et al.*<sup>6</sup> published a theoretical analysis of field enhancement in two-dimensional triple junctions. Due mathematical complexities involved, these methods may not extended to practical grid geometries easily. Numerical methods need to be adapted for studying complex geometries.

Equipotential distribution close to the boundary between the ceramic and vacuum using the POISSON code and MAFIA (Solution of Maxwell's equations using a finite integration algorithm) plots of the field distribution found close to the surface of the ceramics obtained were studied<sup>2</sup>. For positive voltages applied to the rear surface of the ceramic, a strong electric field is obtained close to the triple point. It is sufficient magnitude ( $\sim 50 \text{ MV/m}$ ) to allow field emission from the surface of the metallic grid.

Park *et al.*<sup>7</sup> used ANSYS finite element software for studying the effect of thickness of ferroelectric material and upper electrode diameter on polarization switching and electron emission of  $\text{Pb.Zr}_{0.8}\text{Ti}_{0.2}\text{O}_3$  ferroelectric cathode. They found that variation of the grid electrode width almost did not affect the potential distribution for the given thickness but an uneven potential distribution region near the grid electrode was enlarged with increasing ferroelectric thickness. Flechtner<sup>8</sup> has carried out electrostatic simulation

\*Corresponding author (E-mail: mravi@mtrdc.drdo.in)

using POISSON, a subset of SUPERFISH codes. His work shows that a DC voltage of the same magnitude as the peak of the voltage pulse will produce an electric field at the edges large enough to cause field emission. Shur *et al.*<sup>9</sup> carried out simulation of static potential distribution at the cathode surface using the partial differential equation (PDE) toolbox for MATLAB, which realizes the finite element numerical techniques. They attributed wide electron energy spectrum measured to the surface potential distribution. Carleton<sup>10</sup> used Integrated Software's Electro 2D v5.1 software to determine the local field and potential distributions through the thickness of the ferroelectric cathode. The software uses the Boundary Element Method.

As a summary of reported literature we can say, the grid electrode on the emitting surface of the ferroelectric cathodes changes the applied field distribution. The grid induces both the normal and tangential components. The normal field, which may cause polarization switching or field enforced phase transition is negligibly small near the ferroelectric surface uncovered by the grid. Hence, polarization switching or field-induced phase transition can occur in the vicinity of grid where electric field is sufficiently large. The tangential electric field component appears near the electrode strips in typical ferroelectric cathode geometry. The tangential electric field may cause acceleration of electrons along the ferroelectric surface with subsequent electron avalanching and surface plasma generation. Besides, the tangential electric field component near the electrode strips may cause 90° domain switching in PZT ceramics<sup>1</sup>.

Strong electron emission from current densities  $\sim 100 \text{ A/cm}^2$  is always associated with surface plasma generation. Shur *et al.*<sup>11</sup> showed that there was plasma on the surface of paraelectric PLZT 12/65/35 phase. Dunaevsky and Fisch<sup>12</sup> have studied surface discharge on Pz27 produced by Ferroprem. Mesyats<sup>13</sup> studied the plasma creation on the surface of BaTiO<sub>3</sub> under the application of HV nanosecond pulses. He suggested that electron emission from triple points forms the plasma. In another communication, Shur *et al.*<sup>9</sup> presented the plasma assisted electron emission PLZT 7/65/35 cathode. They showed that primary electron emission required for surface flashover initiation may arise due to either field emission from triple junctions or electron emission caused by polarization reversal.

These primary electrons then can multiply as they traverse along the surface due to tangential component of the electric field due to secondary electron emission from ferroelectric cathode surface. From the above discussion, it is clear that the electric field enhancement at the triple point junctions due grid electrode and ferroelectric material combination, can initiate surface plasma. This mechanism does not involve any ferroelectric properties of materials except for the high dielectric constant of the PLZT materials. Though plasma can also be initiated by polarization reversal in ferroelectric phase, here only plasma assisted electron emission from ferroelectric cathodes in non-reversal mode is discussed. It is very essential to understand the factors, like grid electrode thickness, shape, thickness and dielectric constant of ferroelectric materials, etc, influencing the triple point electric field before the plasma formation

## 2 Method of Simulation

ANSYS electric module is used for modeling of FE cathodes. The basic geometry that was modeled in this study is depicted in Fig. 1. The emitting surface of the ferroelectric cathode is covered with a grid. The width of grid vanes is  $W$  and the gap between the consecutive vanes is  $g$ . The thicknesses of the grid and the ferroelectric material are  $t_g$  and  $d$ , respectively. Anode to cathode gap is defined as  $d_{AK}$ . Considering the symmetry of the problem, two dimensional analysis of only one cell has been carried out. Typically, both strip width and the distance between the strips of the grid are 200  $\mu\text{m}$ . Generally, pulse voltage is applied in such a way that the electric field is more than 20 kV/cm for both reversal as well as non-reversal modes of ferroelectric emission. In the simulation, it is assumed that all the interfaces under consideration are ideal ones, i.e., clean, exact and elaborate contact is achieved between the grid and the ferroelectric surface.

For the simulation work carried out to understand the effect of dielectric layer, model shown in Fig. 2 is

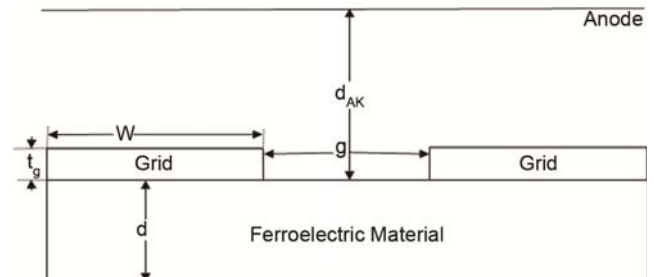


Fig. 1 — Schematic diagram of ferroelectric cathode model.

used. Thickness of the grid is taken as 10  $\mu\text{m}$ . The thickness ( $d_i$ ) of the dielectric layer is considered as 2  $\mu\text{m}$  and dielectric constant is taken as 5. The distance between the anode and the grid 100  $\mu\text{m}$  and thickness of the ferroelectric sample is 90  $\mu\text{m}$ . Length of the ferroelectric along the  $x$ -axis is 400 microns. Boundary conditions used in the problem are grid electrode and the anode is maintained at 0 V. A voltage is applied on the rear side of the ferroelectric material to create a field of 20 kV/cm. The dielectric constant of the ferroelectric is taken as 1000 in the analysis.

### 3 Results and Discussion

#### 3.1 Results without dielectric layer

The potential distribution results for a thickness of 10  $\mu\text{m}$  are shown in Fig. 3. Each solid line presents an equipotential line, and the potential difference between each single line is about 11% of the applied voltage. The equipotential lines under the grid electrode started to bend near the electrode edge, and extended into the vacuum region. Crowding of equipotential lines near the triple point junction indicates that the electric field is maximum at the triple point junction.

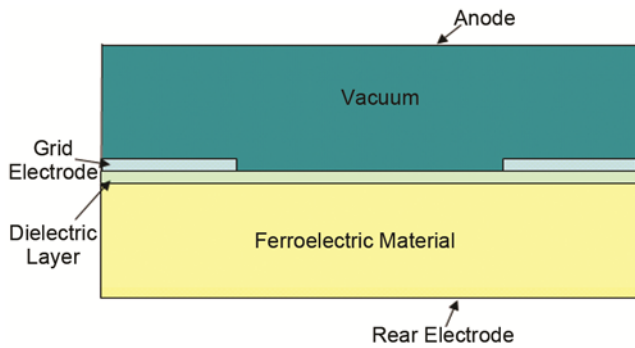


Fig. 2 — Schematic diagram of FE cathode with dielectric layer on the emitting surface below the grid.

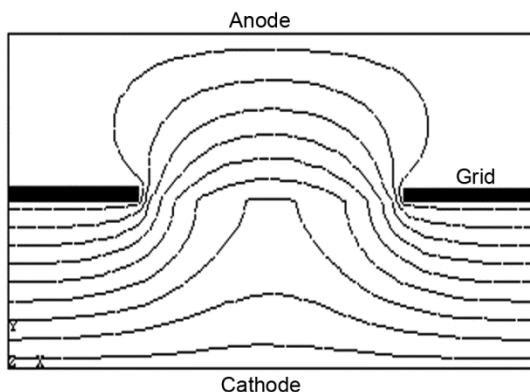


Fig. 3 — Potential distribution with 10 microns grid thickness.

Figure 4(a,b,c) present the field parallel to the surface ( $E_x$ ), the field normal to the surface ( $E_y$ ), and the scalar value ( $E_{sum}$ ) of the vector summation of  $E_x$  and  $E_y$ , respectively. These values of  $E_x$ ,  $E_y$  and  $E_{sum}$  are the values on the emitting surface of the ferroelectric cathodes. As shown in Fig. 4(a), the tangential electric field  $E_x$  increased abruptly at the electrode edge and decreased gradually at the bare ferroelectric surface. At the region middle of the two

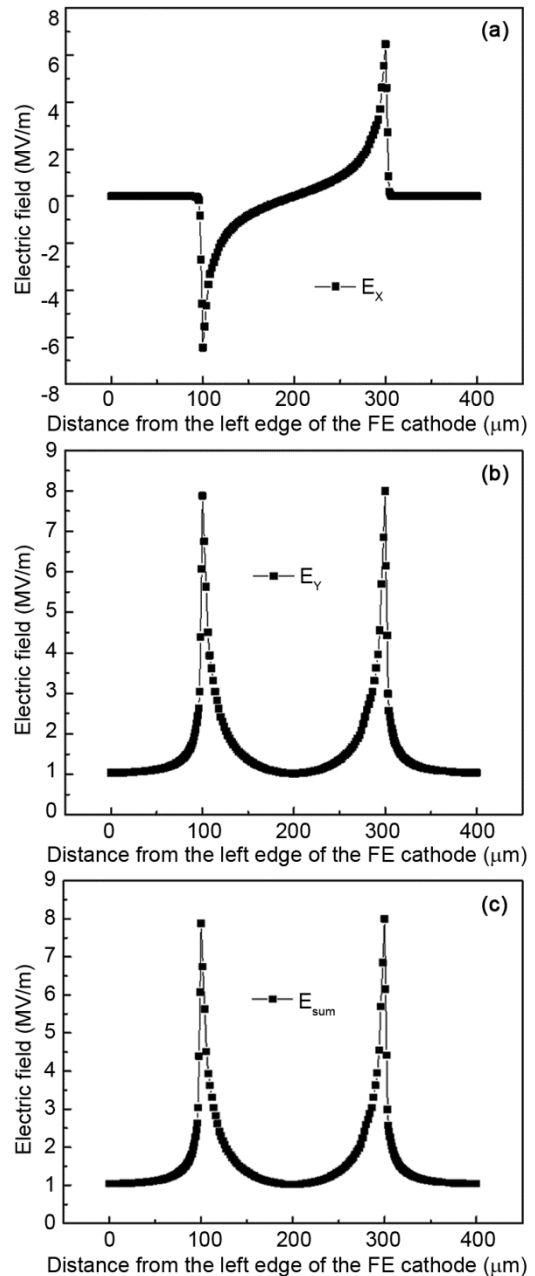


Fig. 4 — Electric field distribution of the emitting surface along the distance from the left edge of the ferroelectric cathode (a)  $E_x$ , (b)  $E_y$ , and (c)  $E_{sum}$ .

grid electrode, the tangential field became zero. Normal field value is 4.5 kV/mm ( $4.5 \times 10^7$  V/m) near the triple junction point and then decreased below the applied field ( $E_0$ ) value of 2 kV/mm at the bare ferroelectric surface between grid electrode. In this region, almost the whole potential drops on the vacuum. The variation of normal electric field along the thickness of the ferroelectric cathode is shown in Fig. 5.  $E_y/E_0$  is plotted as a function of distance from the triple point junction at different depths from the emitting surface of the ferroelectric cathode.  $E_y/E_0$  value initially falls rapidly as the distance from the grid electrode increases and then the rate of decrease becomes very small. From this, it may be concluded that the polarization reversal may be difficult at the bare ferroelectric surface as the electric field values are very small in this region.

Theoretical expression for the potential distribution<sup>4,6</sup> at the triple point depends on the curvature of the field ( $\nu$ ). It can be determined by imposing the boundary conditions for potential ( $\Phi$ ) and  $D\Phi$ . The resulting expression, from which we can determine the value of ( $\nu$ ), is:

$$\varepsilon_r \tan(\nu(\pi - \alpha)) = -\tan(\nu\alpha) \quad \dots (1)$$

where  $\varepsilon_r$  is the dielectric constant of the ferroelectric material and  $\alpha$  is the angle of the ideal conducting edge at the triple point junction.

Surface plasma on ferroelectric cathode has been observed by many researchers. Under the influence of unipolar electrical pulses, this is likely to cause extensive erosion of the metallic grids on the cathode emitting surface. Rosenman *et al.*<sup>14</sup> in their experiments on electron emission from Y-cut ferroelectric triglycine sulfate (TGS) plates, used a

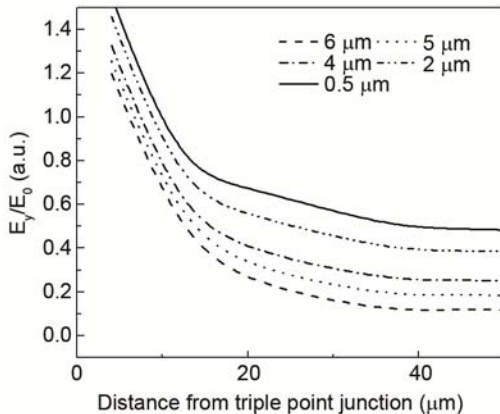


Fig. 5 — The normal electric field  $E_y/E_0$ , as function of distance from the grid electrode for different depths from the emitting surface of FE cathode.

copper fine grid  $\sim 4 \mu\text{m}$  wire diameter and  $17 \mu\text{m}$  periods. After the emission test it has been observed in XPS analysis that the presence of copper material from the grid electrode on the crystal surface. Kovaleski<sup>15</sup> observed that the ferroelectric cathode was heavily damaged after 5000 unipolar voltage pulses. He also used different grid materials like, molybdenum, silver paint and Mo thin films. One of the interesting observations in this paper is that more current density at lesser anode bias has been obtained from APC 857 ferroelectric cathode with silver paint electrodes than the from the cathode of same material with 0.38 mm thick molybdenum grid. Emission area, diode gap and configuration of testing are same in both the cases. Also from the experiments carried out in the laboratory it has been observed that damage of grid is originating from the triple points. It is hence necessary to design the grid on the emitting surface properly for achieving long life and good emission density.

Simulation was carried out to understand the effect of grid thickness using the model discussed above. Thickness,  $t_g$  of the grid is varied to see its effect on the triple point electric field. Boundary conditions used in the problem are grid electrode and the anode is maintained at 0 V. A voltage is applied on the rear side of the ferroelectric material to create a field of 20 kV/cm. The dielectric constant of the ferroelectric is taken as 1000 in the analysis.

As discussed by Takuma<sup>16</sup>, value of  $\nu$  is zero for  $\alpha$  is  $0^\circ$  and  $90^\circ$ . He showed that there would be no field enhancement at triple junction when the angle between the dielectric and metal is  $90^\circ$ . Similar result was derived by Chung *et al.*<sup>17</sup> also. However when the thickness of the grid is smaller compared to the ferroelectric thickness it is observed in the simulation that there will be an increase in the triple junction electric field. When the grid thickness is increased beyond 10 microns, the triple junction field starts reducing and approaching toward the ideal case of no field enhancement. The variation of normalized  $E_{\text{sum}}/E_0$  with grid thickness is shown in Fig. 6. This increase in the triple point electric field for thin grid also explains the higher emission achieved from APC 857 with silver paint electrodes than with 0.38 mm thick molybdenum grid. However too thin grid may be damaged very fast when operating under surface plasma generations for strong electron emission.

The electric field magnitude  $E$  near the triple point in vacuum as function of distance  $r$  from the triple

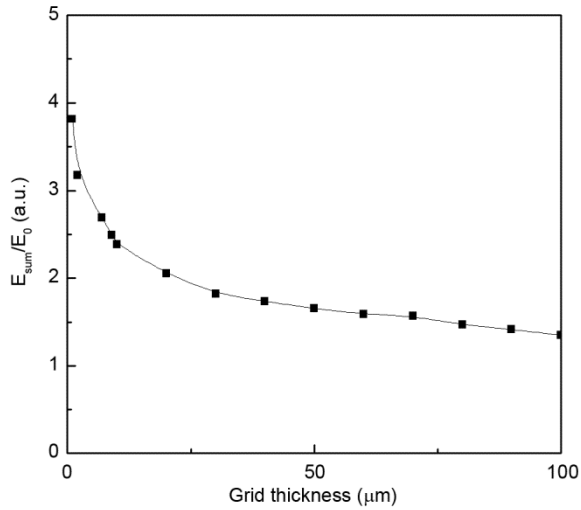


Fig. 6 — Variation of  $E_{\text{sum}}/E_0$  with grid thickness.

point<sup>4,17</sup> is given by  $E = A_1 \nu r^{\nu-1}$  where  $A_1$  is a constant and  $\nu$  is curvature of the field. For large dielectric constants ( $\epsilon_r \rightarrow \infty$ ), the curvature approaches the value 0.5. It implies that electric field has to approach towards its limiting value as dielectric constant is increasing towards infinity. To verify this, simulation has been carried out with different values of dielectric constant ( $\epsilon_r$ ). Same geometry shown in Fig. 1 has been used. The grid thickness is kept constant at 10  $\mu\text{m}$ . The value of  $\epsilon_r$  is changed from 1 to 500. The simulation results are shown in Fig. 7 and it can be inferred that value electric field approaches its limiting value when  $\epsilon_r$  value increase beyond 50. These results are consistent with the reported results in the literature<sup>17</sup>. Hence, as mentioned earlier, the value dielectric constant is taken 1000 in all simulations carried out.

### 3.2 Results with dielectric layer

Triple point electric field in the typical ferroelectric configuration approaches towards its limiting value even the dielectric constant increased considerably. Only way to increase the triple junction electric field is to increase the voltage pulse value applied to the rear of the ferroelectric material. However, this will lead to more residual stress in ferroelectric material and eventually may lead to fracture of it. It is important to increase the triple junction electric field without increasing the applied field. Electrons emitted via field emission can initiate surface flashover. Dunaevsky *et al.*<sup>12</sup> pointed out that the initial stage of the surface flashover is the development of a saturated SEE avalanche. They measured the secondary

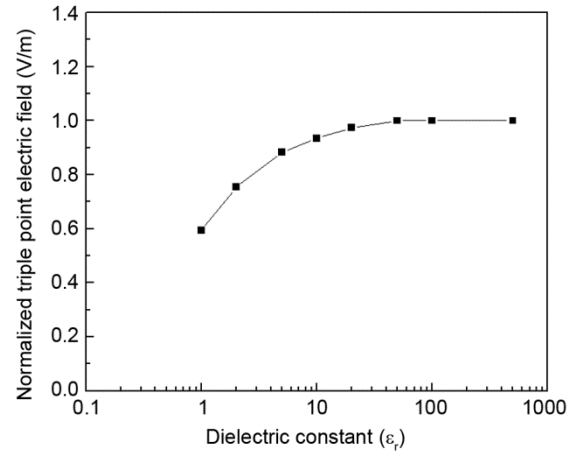


Fig. 7 — Variation of normalized triple point field with dielectric constant.

electron emission coefficient of Pz27, commercially available from Ferroperm. They found that at energies of primary electrons between 20 and 100 eV, the yield of SEE from Pz27 was found considerably higher than the one from boron nitride and other conventional dielectric materials like alumina ceramics, Macor, and Teflon. According to Schachter<sup>4</sup>, the current emitted via field emission at the triple junction is proportional to the dielectric constant. A low dielectric constant film between the ferroelectric and the grid electrode can enhance the triple junction electric field and at the same time reduce the secondary electron coefficient thereby minimizing surface plasma generation. In this case, major contribution for current may come from field emission though the role of surface plasma cannot be ruled out. Studies on the ferroelectric cathodes with a dielectric layer of low dielectric constant sandwiched between the grid electrode and the ferroelectric material have been carried out. The interface between the two dielectrics lies on an equipotential surface.

Potential distribution of the ferroelectric cathode with dielectric layer is shown in Fig. 8. It can be seen from the figure that that potential field lines are crowded in top dielectric layer and thereby increase the electric field values in the region. Each solid line presents an equipotential line, and the potential difference between each single line is about 11% of the applied voltage. Though no ferroelectric property of the sample is utilized in the simulation carried out except for its high dielectric constant, it is referred as ferroelectric to differentiate between the top layers with low dielectric constant. The potential across the ferroelectric materials is almost constant.

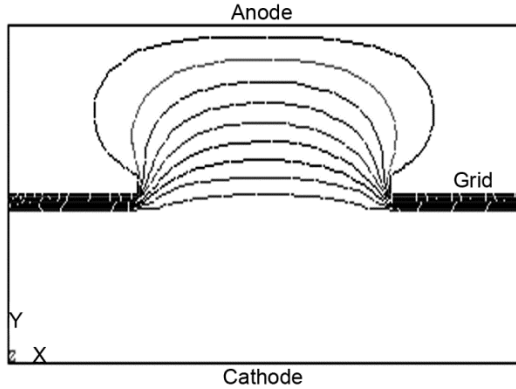


Fig. 8 — Potential distribution with a dielectric layer ( $\epsilon_r = 5$ ) of 2  $\mu\text{m}$  thick.

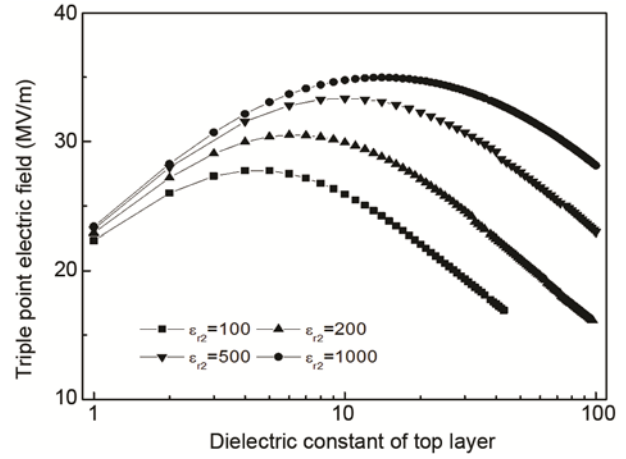


Fig. 10 — Variation of triple junction electric field with dielectric constant (thickness of dielectric layer is 10 microns).

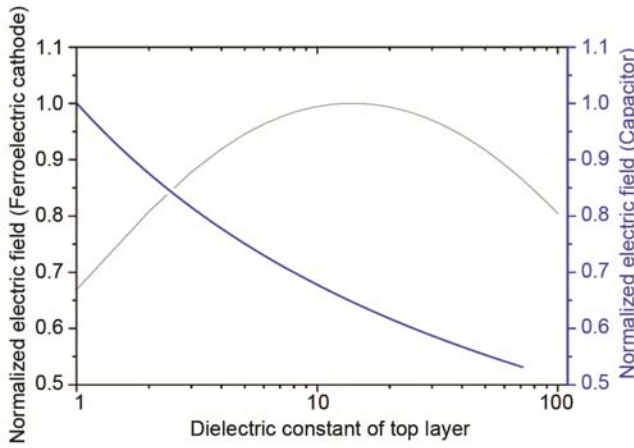


Fig. 9 — Variation of triple junction electric field with dielectric constant in ferroelectric cathode and multi layer capacitor (thickness of dielectric layer is 10 microns).

Variation of triple junction electric field in a ferroelectric cathode and the variation of electric field inside multilayer capacitor as a function of dielectric constant is shown in the Fig. 9, In a two-layer capacitor electric field intensification in the lower dielectric constant material, is maximum at  $\epsilon_{r1} = 1$  and then it is decreasing with increase in dielectric constant<sup>18</sup>. However due the presence of grid structure in ferroelectric cathodes, allowing potential to leak into the vacuum, the triple junction electric field value initially increases up to a particular value of  $\epsilon_{r1}$  and then lowers with further increase of dielectric constant. Triple junction electric field can be optimized by proper choice of thickness and dielectric constant of the top layer depending on the dielectric constant of ferroelectric material. Figure 10 shows the variation of triple junction electric field as function of dielectric constant of the top layer for different dielectric constants of the ferroelectric material. It can

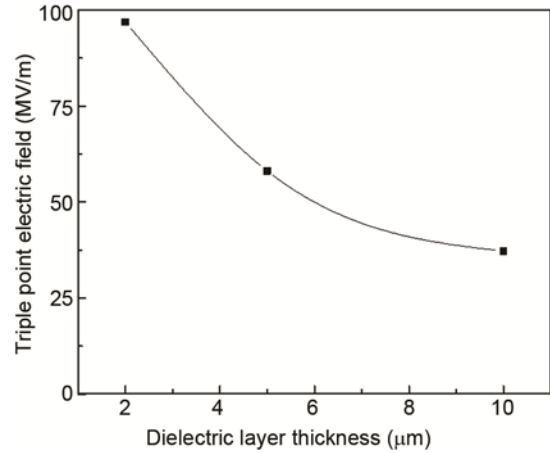


Fig. 11 — Variation of triple junction electric field with dielectric layer thickness (dielectric constant= 5).

inferred that dielectric constant of the top layer for maximum triple junction field increases with dielectric constant of the ferroelectric material.

To understand the effect of thickness of dielectric layer analysis carried out at three different thicknesses of dielectric layer 2, 5 and 10  $\mu\text{m}$  keeping the dielectric constant of the top layer constant at 5. As seen from the Fig. 11, the electric field values are decreasing with increasing dielectric layer thickness.

Figures 12 and 13 present the field parallel to the surface ( $E_x$ ), the field normal to the surface ( $E_y$ ). As shown in Fig. 12, the tangential electric field  $E_x$  increased and decreased abruptly at the electrode edge and zero on the dielectric surface. In ferroelectric cathode without dielectric layer,  $E_x$  decreases gradually and becomes zero only at the midpoint between the two electrodes. With dielectric layer, normal field value  $65 \times 10^6$  V/m near the triple

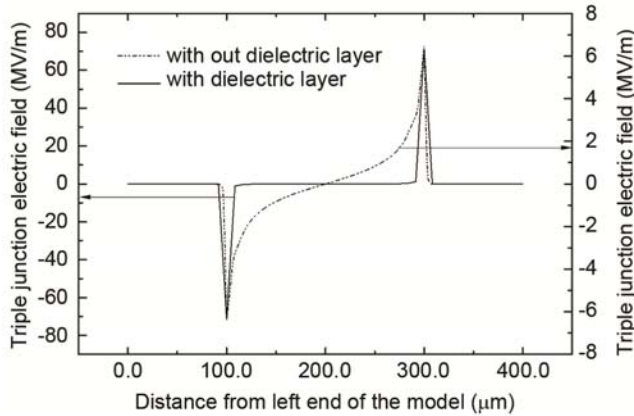


Fig. 12 — Variation of parallel component of electric field along the surface of ferroelectric cathode with and without dielectric layer.

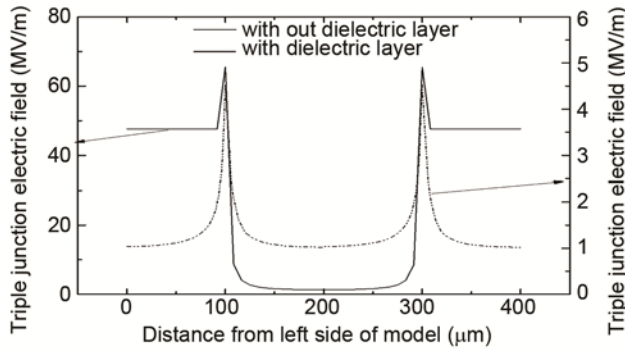


Fig. 13 — Variation of normal component of electric field along the surface of ferroelectric cathode with and without dielectric layer.

junction point as shown in Fig. 13 and then decreased below the applied field ( $E_0$ ) value of  $2.0 \times 10^6$  V/m at the bare dielectric surface between grid electrodes. The marked difference in the normal field distribution is that the  $E_y$  values at the middle of the electrodes are one order smaller than the  $E_y$  just below the electrodes. In the case of FE cathode without dielectric coating the normal component of the field are having same values at locations below the electrodes and at the middle of the electrodes.

Also, the total electric field (vector sum of  $E_x$  and  $E_y$ ) at the triple point junction is  $97 \times 10^6$  V/m, which is about 45 times the applied field value. This large field enhancement can be understood from electric field inside a parallel plate multilayer dielectric capacitor, in which for the same values of dielectric constant and thickness of the top layer, the electrical field inside that dielectric will be  $91 \times 10^6$  V/m, which is of the same order of the triple junction electric field. In case of cathode configuration, electrical flux

will leak in the vacuum due to gap between the grid electrodes. The electric field value just below the grid electrode away from the triple point junction, in cathode configuration is  $47 \times 10^6$  V/m which is approximately half the value predicted parallel plate multilayer dielectric capacitor.

The marked difference in the normal field distribution is that the  $E_y$  values at the middle of the electrodes are one order smaller than the  $E_y$  just below the electrodes. In the case of FE cathodes without dielectric coating the normal component of the field are having same values at locations below the electrodes and at the middle of the electrodes.

The ratio ( $\beta$ ) of  $E_x$  and  $E_y$  is 1.42 in case of ferroelectric cathode without dielectric layer and 1.09 in case of cathode with dielectric layer. Reduced  $\beta$  will result in reduced landing energy of primary electrons<sup>19</sup>. Also for same total triple junction electric field,  $E_x$  is small in case of ferroelectric cathode with dielectric layer. This can reduce the desorption of neutrals<sup>12</sup>.

#### 4 Conclusions

The electric field distributions were calculated for different grid electrode thicknesses and dielectric constant of ferroelectric materials. Equipotential lines under the grid electrode started to bend to ferroelectric surfaces near the electrode edge, and extended into the vacuum region. Increase of the grid electrode thickness reduces the triple junction electric field. Triple junction electric field approaches its limiting value when  $\epsilon_r$  value of ferroelectric material increases.

When a dielectric layer is introduced between the ferroelectric material and the grid, there is an increase the triple junction electric field. The triple junction electric field is more than 48 times the applied field. This structure not only enhances the triple junction electric field but it also changes the  $E_{\parallel}$  (or  $E_x$ ) and  $E_{\perp}$  (or  $E_y$ ) ratio ( $\beta$ ) favorably. Dielectric constant and thickness of the top layer have to be optimized for maximizing the triple junction field. PZT ferroelectric cathode coated with MgO thin film has shown stable and enlarged cycles of electron emission<sup>20</sup>. Further studies on role dielectric layer on the plasma formation in ferroelectric cathodes needs to be studied.

#### Acknowledgement

The authors are thankful to Director, MTRDC for his encouragement and permitting us to publish this work.

**References**

- 1 Rosenman G, Shur D, Krasik Y E & Dunaevsky A, *J Appl Phys*, 88 (2000) 6109.
- 2 Fleddermann C B & Nation J A, *IEEE Trans Plasma Sci*, 25 (1997) 212.
- 3 Nation J A, Schachter L, Mako F M, Len L K, Peter W, Tang Cha-Mei & S R Triveni, *Proc IEEE*, 87 (1999) 875.
- 4 Schachter L, *Appl Phys Lett*, 72 (1998) 421.
- 5 Heydari H & Tille T, *Proceedings of the particle accelerator conference*, (1997) 2784.
- 6 Chung M S, Choi T S & Yoon B G, *Appl Surf Sci*, 251 (2005) 177.
- 7 Park J, Kim Y T & Yoon K H, *J Appl Phys*, 91 (2002) 1458.
- 8 Flechtner D, *Electron emission and beam generation using ferroelectric cathodes*, Ph. D. Thesis, (Cornell University), 1999.
- 9 Shur D & Rosenman G, *J Phys D: Appl Phys*, 32 (1999) 29.
- 10 Carleton E J, *Thin electrode surface flashover behavior and method for the enhancement of switched polarization in ferroelectrics*, Masters Thesis, University of Missouri, Rolla, 2000.
- 11 Shur D, Rosenman G, Krasik Y E & Kugel V D, *J Appl Phys*, 79 (1996) 3669.
- 12 Dunaevsky A & Fisch N J, *Phys Plasma*, 11 (2004) 2957.
- 13 Mesyats G A, *IEEE Trans Dielectr Electr Insul*, 2 (1995) 272.
- 14 Rosenman G, Shur D, Garb K, Cohen R & Krasik Y E, *J Appl Phys*, 82 (1997) 772.
- 15 Kovaleski S D, *Ferroelectric emission cathodes for low-power electric propulsion*, NASA Report, No NASA/CR-2002-211872.
- 16 Takuma T, *IEEE Trans Dielectr Electr Insul*, 26 (1991) 500.
- 17 Chung M S, Hong S C, Cutler P H, Miskovsky N M, Weiss B L & Mayer A, *J Vac Sci Technol B*, 24 (2006) 909.
- 18 Arora R & Mosch W, *High voltage and electrical insulation engineering*, (John Wiley & Son, Inc: New Jersey), 2011.
- 19 Liu Y S, Zhang G J, Zhao W B & Yan Z, *Appl Surf Sci*, 230 (2004) 12.
- 20 Zhu H, Okuyama M, Orikawa Y & Ricinschi D, *Ferroelectrics*, 239 (2000) 389.